PUBLS. INST. GEOPHYS. POL. ACAD. SC., M-29 (395), 2006

# Electric Resistivity Variations of Rock Formation at an Abandoned Mining Shaft Site

Andrzej KOTYRBA, Łukasz KORTAS and Sławomir SIWEK

Central Mining Institute
Pl. Gwarków 1, 40 166 Katowice, Poland

A b s t r a c t

Abandoned shafts, even if backfilled, create a potential hazard for the environment and safe use of post-mining lands. The hazardous phenomena depend on the shaft tube structure and the extent of mining activity in the vicinity and, on the other hand, the dynamic processes which occur within rock strata. Among the processes which affect the rock mass structure is the rainfall water migration and erosion. The amount and rate of water flow within soil and bedrock in the specific area depend on time. The water saturation in rock formation is the main factor which determines the electric properties of geological environment. These phenomena can be used for monitoring erosion processes by electroresistivity or conductometric measurements. In the paper, experimental results of the tests carried out in an abandoned shaft site are described. The tests were performed in three series of measurements conducted using vertical electroresistivity sounding method (VES) in autumn, winter and spring. The results indicate significant changes of rock formation resistivity values due to change in seasonal conditions. This impacts the interpretation of the data collected in geoelectrical measurements.

## 1. Preface

The electroresistivity method uses variations in electrical properties of geological medium to visualize the geological strata arrangement and medium structure. The parameter obtained from the field data in this method is the apparent electrical resistivity $\rho_p$ of the rocks (the reverse of electrical conductivity $\sigma$) as a function of the interval/spacing AB between the current electrodes. The measured values of the parameter depend on the real values (specific resistivity, depth) and could be calculated using inversion methods. The voids in the dry rock layers are the elements that cause strong positive anomalies in the visual representation of the data recorded in electroresistivity

measurements. Water filled-voids generate negative anomalies. For these reasons, the electroresistivity method is applied to detect and localize the voids of different origin in rock formations and in particular the old shafts. In this application of the method, measurement data characterize a geological medium for a definite moment of time (stationary case). The electrical properties of this medium are mainly affected by water content due to seasonal changes. Due to low compaction of the material used for shafts backfilling, the ground surface in such sites could always become unstable. The possibility of vertical electroresistivity sounding (VES) method application for subsidence hazard monitoring in time domain was the aim of tests conducted in the Triassic carbonate massif in a site located in Olkusz region (Poland). In this nonstationary (time dependent) case, the measurement data strongly depend on water content in the surveyed geological strata.

## 2. Resistivity of Porous Media with Fluctuating Water Content

In theoretical approach, the resistivity of porous media, where part of pores are filled with water of resistivity $\rho_w$, can be expressed by Archie's formula (Militzer *et al.* 1978)

$$\rho = F \cdot \rho_w \cdot \delta^n , \tag{1}$$

where: $F = a\, p^{-m}$ ; $a$, $m$, and $n$ are empirically found parameters; $p$ is the fractional pore volume parameter ($V_p/V$); $\delta$ is the fraction of pore volume filled with water ($V_w/V_p$); and $a$ is the formation factor. Empirical values of $a$, $m$ and $n$ for dolomite and limestone can be taken as follows: $a$ = 0.6–0.8 (coarse grained – fine grained); $m$ = 2.15–2.30 (coarse grained – fine grained); $n$ = 1.3–2.2.

Formula (1) determines the static case in which parameters $\rho$ and $\delta$ are time independent. In a dynamic case, both parameters depend on time. Therefore, formula (1) can be written in the form:

$$\rho(t) = F \cdot \rho_w \cdot \delta^n(t) . \tag{2}$$

Performing temporary measurements at a specific site we gather data sets which can be expressed in the form:

$$\begin{aligned} &\rho_1(t_1) = F \cdot \rho_w \cdot \delta_1^n(t_1) \\ &\rho_2(t_2) = F \cdot \rho_w \cdot \delta_2^n(t_2) \\ &\rho_3(t_3) = F \cdot \rho_w \cdot \delta_3^n(t_3) \\ &\ldots \\ &\rho_i(t_i) = F \cdot \rho_w \cdot \delta_i^n(t_i) . \end{aligned} \tag{3}$$

If we neglect the mass transport within the shaft tube (**case 1**), it can be assumed that in the test area parameters $F$ (porosity factor) and $\rho_w$ (water resistivity) are constant. Introducing the time dependent fractional parameter $Q_n$, the resistivity changes directly depend on the pore volume filled with water, which can be expressed by the equation:

$$Q_n = \frac{\rho_i(t_i) - \rho_1(t_1)}{\rho_1(t_1)} = \frac{\delta_i^n(t_i) - \delta_1^n(t_1)}{\delta_1^n(t_1)} \ . \tag{4}$$

The above equation reflects in fact the water balance in rock formation. It is free from primary resistivity value of rock formation. The resistivity data sets from the test site can be directly used as the analog of water volume fluctuations, if the quantitative rainfall record is known. The resistivity variations balance should be similar to the water content variations balance. In the case of mass transport in a shaft tube, porosity parameter ($F$) is not constant, which leads to the set of equations:

$$\begin{aligned} &\rho_1(t_1) = F_1 \cdot \rho_w \cdot \delta_1^n(t_1) \\ &\rho_2(t_2) = F_2 \cdot \rho_w \cdot \delta_2^n(t_2) \\ &\rho_3(t_3) = F_3 \cdot \rho_w \cdot \delta_3^n(t_3) \\ &... \\ &\rho_i(t_i) = F_i \cdot \rho_w \cdot \delta_i^n(t_i) \, . \end{aligned} \tag{5}$$

In **case 2** the fractional parameter $Q_n$ is described as

$$Q_n = \frac{\rho_i(t_i) - \rho_1(t_1)}{\rho_1(t_1)} = \frac{F_i \cdot \delta_i^n(t_i) - F_1 \cdot \delta_1^n(t_1)}{F_1 \cdot \delta_1^n(t_1)} \ , \tag{6}$$

$$Q_n = \frac{F_i \cdot \delta_i^n(t_i)}{F_1 \cdot \delta_1^n(t_1)} - 1 \, . \tag{7}$$

In **case 2**, the resistivity fluctuations balance is not equal to water content balance and depends on fractional pore volume parameter $F$. The mass transport in shaft tube disturbs the spatial porosity distribution (parameter $F$), which can be monitored by various techniques of geoelectrical measurements.

## 3. Description of Test Site and Measurements Performed

The vertical electroresistivity sounding method was applied to collect field data in the test site. The measurements were performed in six points called $S_1$ to $S_6$, localized in the studied area as shown in Fig. 1.

The primary goal in the first series of field works (autumn) was to determine the model of geological structure of the tested ground. The secondary goal was to outline the places in which the electrical properties of the Triassic strata are abnormally exaggerated or lowered. Data collected in the next series (winter and spring) were supposed to determine whether and what changes in the resistivity values take place in the test site area. The important issue here was to estimate the shape of anomalous zones during the whole experiment and to specify their possible influence on the assessment of surface stability.

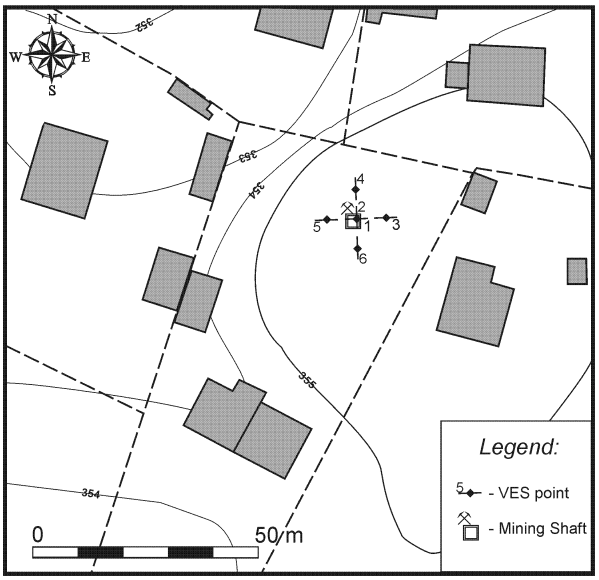


Fig. 1. Location of VES points in the test site.

The electroresistivity soundings $S_1$ and $S_2$ were performed within the precincts of the abandoned shaft and had perpendicular directions. The rest of the soundings ($S_3$–$S_6$) were conducted at 6.5 m distances from soundings $S_1$ and $S_2$ in the following direction: N ($S_4$), S ($S_6$), E ($S_3$) and W ($S_4$). Electrode arrays for soundings $S_1$, $S_3$ and $S_5$ were oriented in direction WNW-ESE, and for $S_2$, $S_4$ and $S_6$ in direction NNE-SSW, which was connected with the existing buildings placement and urban infrastructure. In the points $S_1$–$S_4$, fifteen data points were collected for AB/2 spacing from 1.5 to 72.5 m and in $S_5$ and $S_6$ sixteen data points were measured for AB/2 = 1.5 to 95 m.

The field works were performed with application of digital geoelectric apparatus CMG-01, made in Poland. Altogether during data acquisition process 312 data points were recorded (104 data points in each series). Each value registered by the operator was the average value from a couple of instrument readings.

### *3.1 Geology and mining*

The test area lays in the southern part of the large Tertiary monocline of diversified lithology and tectonics. This formation is strongly cracked and tectonically dislocated. Tectonics of the area has been formed during the Alpine orogenesis in Saxon phase. In that time, the dense net of normal faults has been created. They divided the area into numerous blocks with different displacement and inclination. The prevailing number of faults has azimuths ranges from 10°–30° to 95°–120°. Dislocations in directions NW-SE and NE-SW or NNW-SSE or WSW-ENE are also sometimes observed.

The net of faults belonging to various systems makes separate blocks which are the units of lower level inclined independently of the general direction of the upper

unit throw. The inclination of layers in blocks is conditioned by the faults of the lowest order. The inclination values range from 4°–5° to 20°–40°.

The soils near surface are of anthropogenic origin (mine wastes). Below them, the Quaternary sediments (clays and sands) should be present. They are not seen on VES curves. This is the reason for assuming that in the test site the Triassic sediments are cropping out on the surface, as frequently observed in Olkusz area. They are composed of limestone, marbles and dolomites of the lower and middle Triassic strata. In this formation, the lead and zinc ore bearing veins occur, being the subject of mining exploitation in the past. In Triassic rocks, the carst phenomena are frequently observed.

### *3.2 Water conditions*

Description of water conditions in test site area is based on the hydrographical map elaborated and published in 1987 (Fig. 2). According to this source, the test area lies in Biała Przemsza and its tributaries river basin. Watersheds dividing river basin of Biała Przemsza are of IV$^{th}$ order (i.e. Bobrka, Sztoły, Kozi Bród). Natural water conditions in the area are highly disturbed by mining activity of deep mine Pomorzany

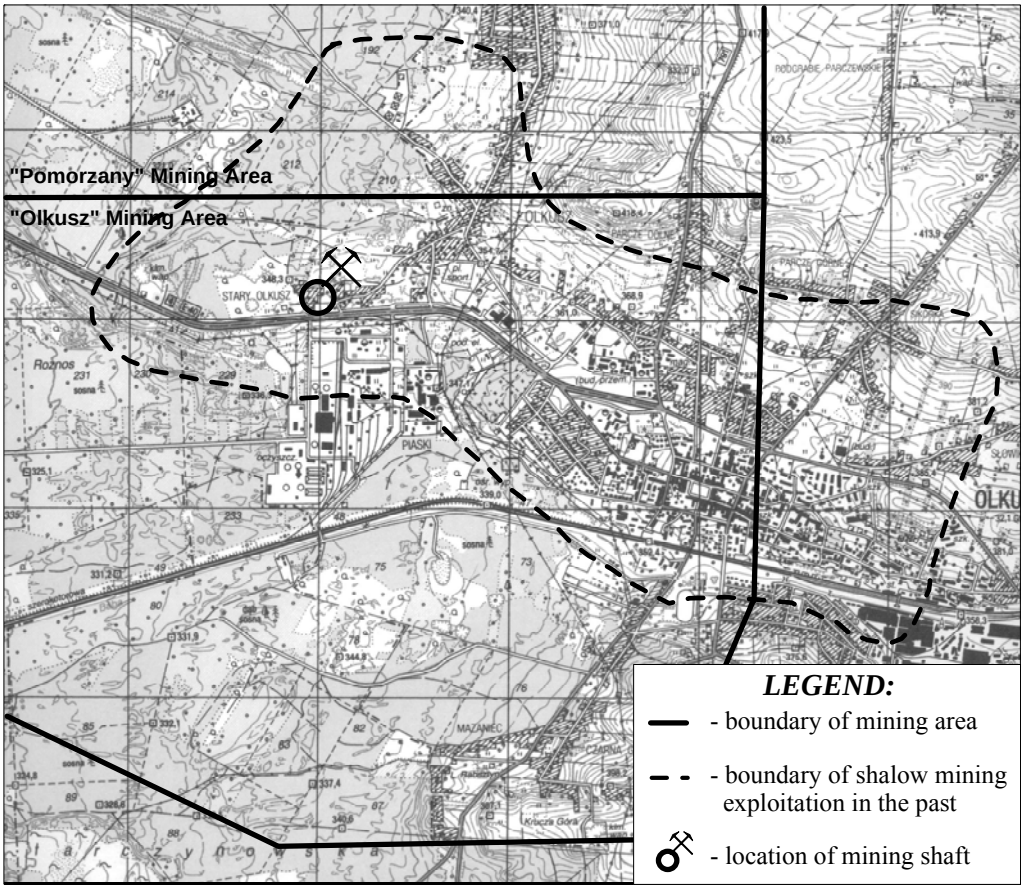


Fig. 2. Test site location on background of topographic map of the region.

(about 1 km to the north) and sand open pit mine Szczakowa (about 6 km to the south). Those mines drain the Quaternary-Triassic water horizon. In the area located to the north from the test site, the water level is lowered approximately to a depth of 100 m b.g.l.

South of the test site, the water level is at a depth of approximately 20 m b.g.l. In the area located on the eastern side of the test site, ground water table is observed at a depth of approximately 10 m b.g.l. The drainage pattern allows to assess that in the test site area the underground water flows generally in northern direction. It is not clear at what depth the water table occurs there. The hydrographical data are too old to estimate the water table depth in the test site, provided that other mines operating in the vicinity of the test site (Olkusz, Bolesław) have been demolished since 1987. This could affect the water conditions and lead to water table recovery in the test site.

The local water conditions in the test site are influenced by rainfall feed and depth of water table in Triassic sediments. Water table divides the bedrock into aeration and saturation zones. The water content in aeration zone is shaped mainly by rainfall. The precipitation rates during the testing period are shown in Fig. 3 (IMGW bulletins 2004-2005).

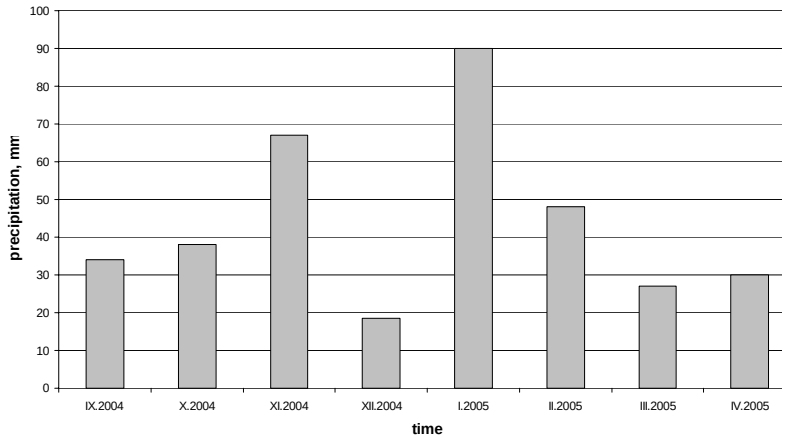


Fig. 3. Precipitation in the test area during testing period (monthly rates).

The percentage of atmospheric rainfalls that infiltrate in the rock formation in Poland ranges between 16 and 25%. The average for Poland is equal to 18.2% (Rogoż 2004). In the active mining areas this percentage is higher and ranges between 30 and 50% (Sztelak 1965). It could be assumed that in the areas where the mining exploitation has ended, this value is still exaggerated in comparison to other regions in Poland and is of the order of 30%.

### *3.3 Hydrogeological Model of Backfilled Shaft*

The common practice of shafts liquidation is to backfill them with waste material from exploitation of ore bearing strata. In ancient mining, the waste material from

digging works was stored on the surface around the shaft. A mass volume excavated exceeded the shaft volume. The stored waste formed an anthropogenic hill. The primary material usually had a high content of cobble fraction. In weathering process only a small part of dolomite or limestone cobbles changed the size, altering to clay and gravel. Therefore, the prevailing part of mining waste remained in the form of coarse rock fraction. This material had substantially higher porosity and related permeability compared to rock basement. After completion of mining works at a specific area, part of the waste has been transferred to the shaft. Due to irregular form of cobbles, it can be assumed that the porosity of backfilling material remained primary, i.e., similar to the material stored on the surface. Nevertheless, underground openings in shaft vicinity enable the processes of washing out and erosion within the backfilling material, by migrating rainfall waters. Those processes are probably responsible for mass transport within old shaft's tube and surface displacements. The acting force of washing out and erosion is dependent on the volume of percolating water, which is time dependent. Therefore, the model depicted in Fig. 3 can be used for water and mass balance analysis.

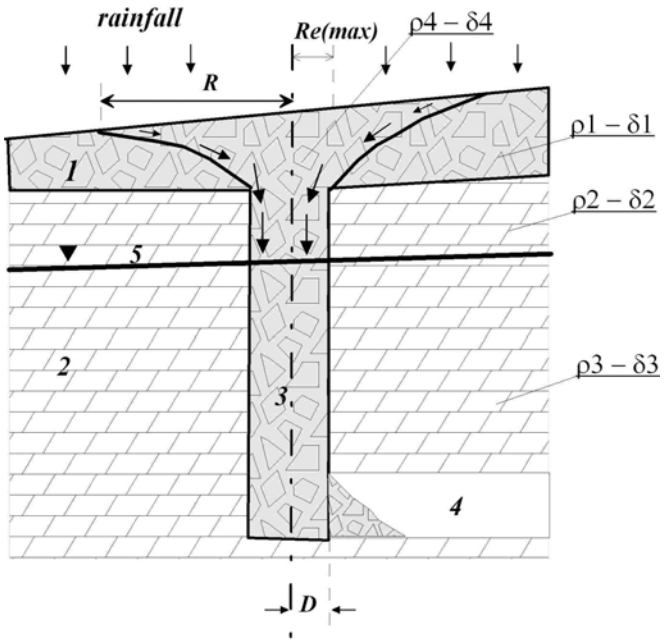


Fig. 4. Hydrogeological model of old backfilled shaft with aeration and saturation zones (1 – waste, 2 – rock basement, 3 – shaft's tube, 4 – mine void, 5 – water table, D – shaft radius, R – radius of local catchment area, Re (max) – radius of zone with maximum water action).

According to the model presented in Fig. 4, an old shaft forms a local catchment area, due to higher permeability of the backfilling material. The power of water erosion and suffusion processes is the highest inside the shaft's tube. The particles eroded or washout from the backfilling material can be transported to the mining voids in the

vicinity (mass transport). It should be noted that the water action is highest in aeration zone. In the case of percolation, the resistivity values ($\rho_i$) of model layers are proportional only to water content ($\delta_i$). The resistivity variations in time should be similar to rainfall rates. In case of mass transport within shaft's tube, the above relation should be disturbed. This finding can be used for prediction of surface displacements, based on continuous or temporary resistivity (conductivity) measurements data, gathered in the site.

## 4. Test Results

Data collected in field measurements ($I$, $\Delta V$) were recalculated to obtain apparent resistivity $\rho$ in each data point of the studied area. Taking this data, the bilogaritmic plots of dependence $\rho$ [Ωm] vs. $AB/2$ (m) called the sounding curves were made. Those plots apart from documenting the conducted measurements are the basic materials for analysis of temporary variations of rock formation electric resistivity as well.

Additionally using Surfer/Golden Software, horizontal contour maps were made showing the distributions of resistivity values in halfspace. A parameter for horizontal cuts was half of the $AB$ spacing of current electrodes. To all plots a point kriging method of interpolation (with parameters shown in Table 1) was used.

Table 1

Point kriging parameters used in interpolation scheme

| Kriging parameters | |
|---|---|
| Number of sectors to search | 1 |
| Max. number of data to be used from all sectors | 5 |
| Max. number of data to be used from each sector | 5 |
| Min. number of data to be used from all sectors (node is blank if fewer) | 1 |
| Blank node if more than this many sectors are empty | 1 |

Sounding curves recorded in autumn, winter and spring series are set in Fig. 5. One can observe that the shape of the plots of all three series is similar and for greater AB spacing depends on the measurement line azimuth. Soundings with azimuth line ESE-WNW in terms of electrical properties show four-layer medium structure of HK type (the last layer on the curve has a low resistivity value). Soundings performed in spreading line NNE-SSW show five-layer medium structure of HKH type (the last layer on the curve has a high resistivity value). This indicates an anisotropy of the electrical properties of deeper parts of rock formation at the test site. Despite those differences, the measured values of electroresistivity on VES curves change in the interval from about 100 to 1800 Ωm.

Analyzing VES curves one can observe that depending on localization they differ in electroresistivity value of subsurface geological layers. While comparing curves

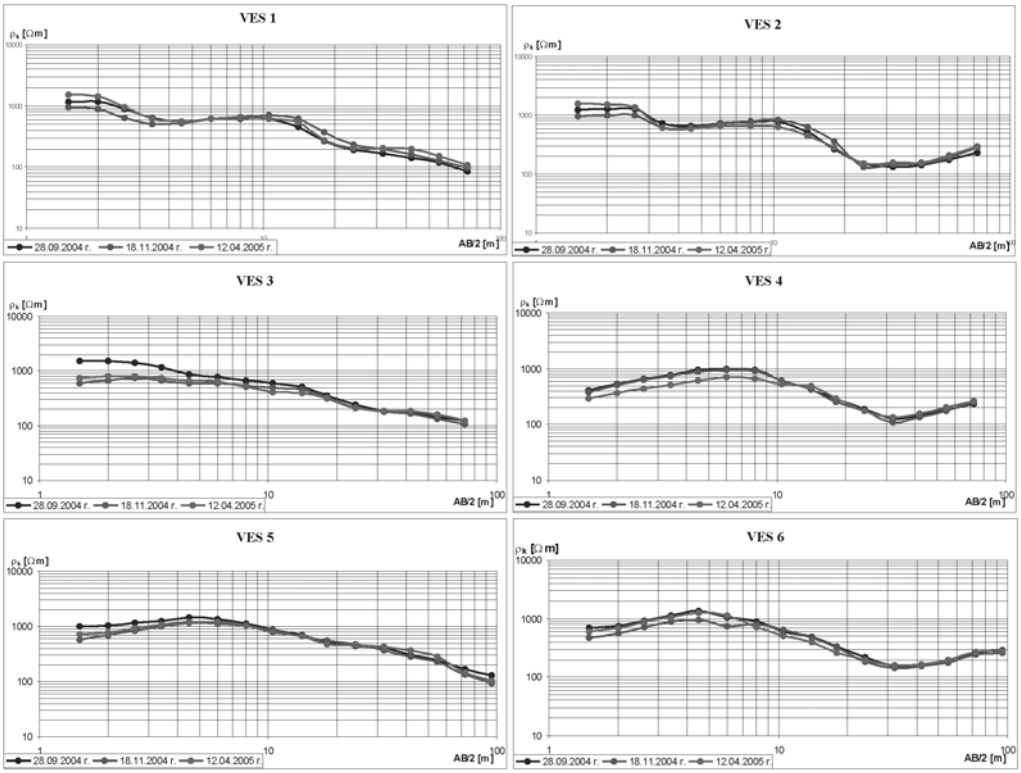


Fig. 5. VES curves $S_1$ – $S_6$. Series: 1 (autumn), 2 (winter), 3 (spring).

for all three series the significant differences are visible also in these parts of the VES plots which correspond to subsurface formations of studied medium (especially plots for $S_3$ and $S_4$). As concerns the medium structure, the VES curves analysis provided the following geoelectrical layers specification (Popiołek *et al.* 2005):

**Layer I** – apparent electroresistivity values range from 700 to 1600 Ωm, depth of deposition 0–1m. Corresponds to the soils in aeration zone.

**Layer II** – apparent electroresistivity values range from 500 to 1500 Ωm, depth of deposition 1–4 m. Corresponds to embankment grounds in aeration zone.

**Layer III** – apparent electroresistivity values range from 300 to 900 Ωm, depth of deposition 4–8 m. Corresponds to position of weathered Triassic rocks in aeration zone.

**Layer IV** – apparent electroresistivity values range from 100 to 300 Ωm, depth of deposition 8–30 m. Corresponds to Triassic rocks formation in saturation zone.

**Layer V** – apparent electroresistivity values range from 100 to 400 Ωm in N-S direction and 100–200 Ωm in W-E direction, depth of deposition > 20 m. Corresponds to Triassic rocks in saturation zone with characteristic cracking pattern with W-E extent.

Because of the fact that geological structure of the substratum is not essential the model calculations in this work were not conducted with application of inversion methods to obtain exact, quantitative interpretation of the VES curves. For the purpose of this work, an approximate estimation is sufficient.

Due to the types of the recorded VES curves (mainly H and K) one can assume that apparent resistivity and depth values given above are close to their real values.

While analyzing the VES curves, an important issue is the remarkable anisotropy of electrical properties of the Triassic rock formations deposited at greater depths in the studied area. The longer axis of the anisotropy ellipsoid extends in N-S direction and is probably caused by tectonics of the rock base of studied area which provide the W-E direction of the layers cracking.

Horizontal contour maps showing distribution of resistivity values of rock formation in series 1, 2 and 3 are illustrated in Figs. 6, 7 and 8, respectively.

At the vertical isoohm sections, a decrease of resistivity values with increasing depth is generally observed. More information about the medium can be obtained from the horizontal isoohm sections analysis. At these pictures positive and negative anomalies connected with the presence of the shaft tube in medium are visible. In the first/autumn series plot the tube is marked in the subsurface strata as a positive anomaly of electroresistivity (AB/2 = 1.5, 2.0 and 2.6) and negative (for spacing AB/2 = 3, 4; 4.5; 6.0 and 8.0 m). In deeper parts of the rock formation, the shaft was not clearly visible but could be localized in the zone of lower values of resistivity.

At the horizontal isoohm pictures of second/winter and third/spring series the shaft tube is marked similarly as at the first/autumn series pictures. The only significant difference concerns the subsurface zone (AB/2 = 1.5; 2.0 and 2.6 m) and is most visible in the data from third/spring series. At the isoohm maps mentioned earlier, the shaft tube is marked as a positive anomaly of resistivity with significant amplitude, which indicates relatively smaller watering of the soil in the tube than the rock. In any case, if we construct contour maps showing relative changes of resistivity between series, the shaft's tube is clearly visible on all pseudo depth levels (Fig. 9).

Comparison of autumn, winter and spring series from qualitative point of view indicates the time variations of electrical properties of the grounds in the studied area. On resistivity contour maps, variations concern the shape, sign and amplitude of the anomaly. The changes are significant in the aeration zone (about 0-8 m b.g.l.). In the formations deposited at the depth that corresponds to saturation zone, the changes of electroresistivity were insignificant. On resistivity change contour maps, the shaft's tube is visible on almost all depth levels. It is well marked especially in the images corresponding to deeper parts of the rock formation.

The analysis of variations shows that in the studied area the backfilled shaft tube plays a role of drainpipe for rainfall water, which infiltrates from the surface down in the medium. Variation in lithology and permeability of the soil used to backfill the shaft helps the tube to play the role of reservoir able to retain rainfall water during the dry periods.

Direct analysis of data sets was performed to obtain quantitative characteristics of the resistivity changes in time interval between each series of measurements. The parameters of analysis are set below:

- The change of resistivity in each sounding point for given AB/2 spacing was calculated in percents: $\frac{\rho_{s2} - \rho_{s1}}{\rho_{s1}} \cdot 100\%$;

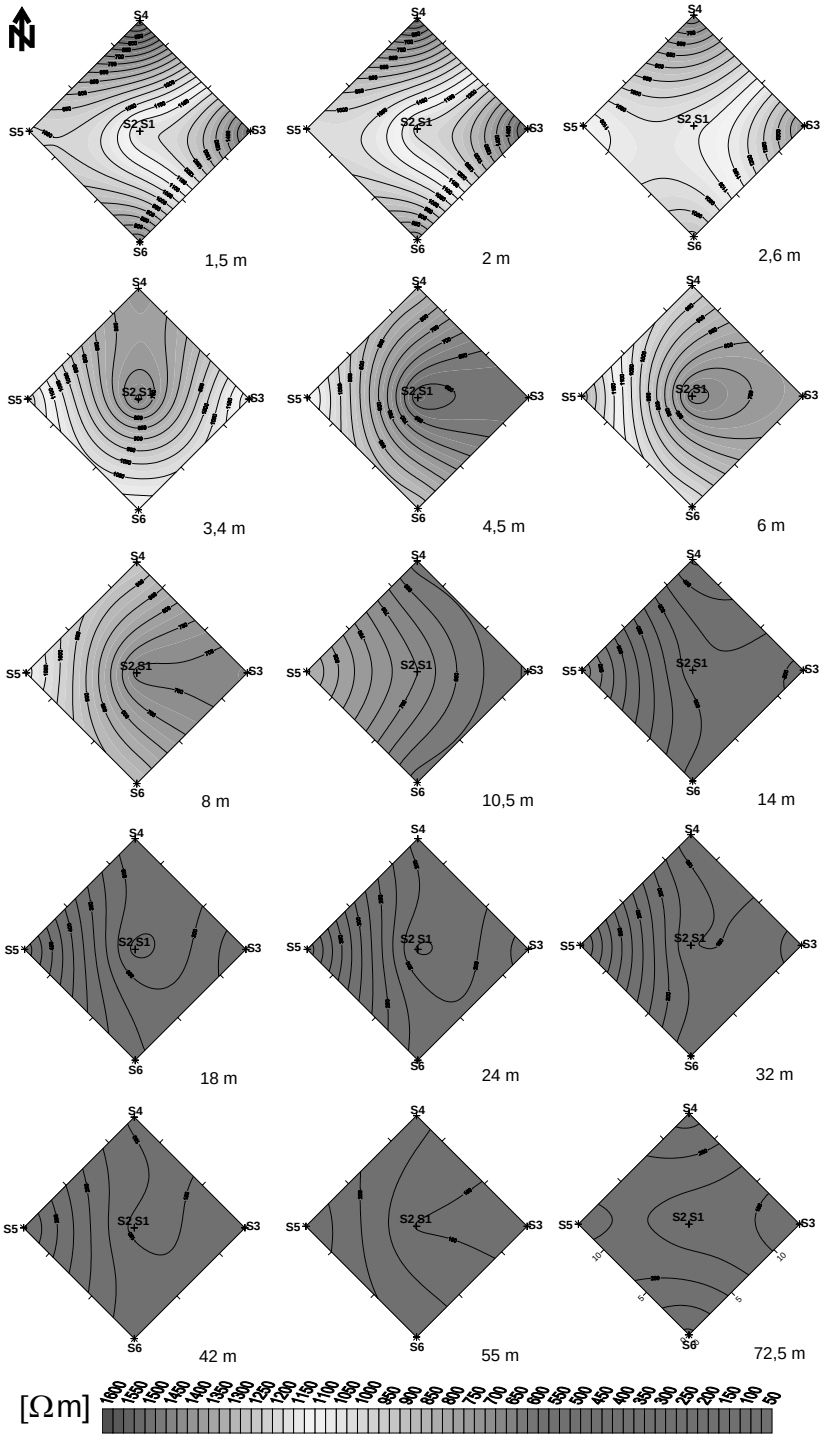


Fig. 6. Resistivity contour maps of the first series of measurements (autumn).

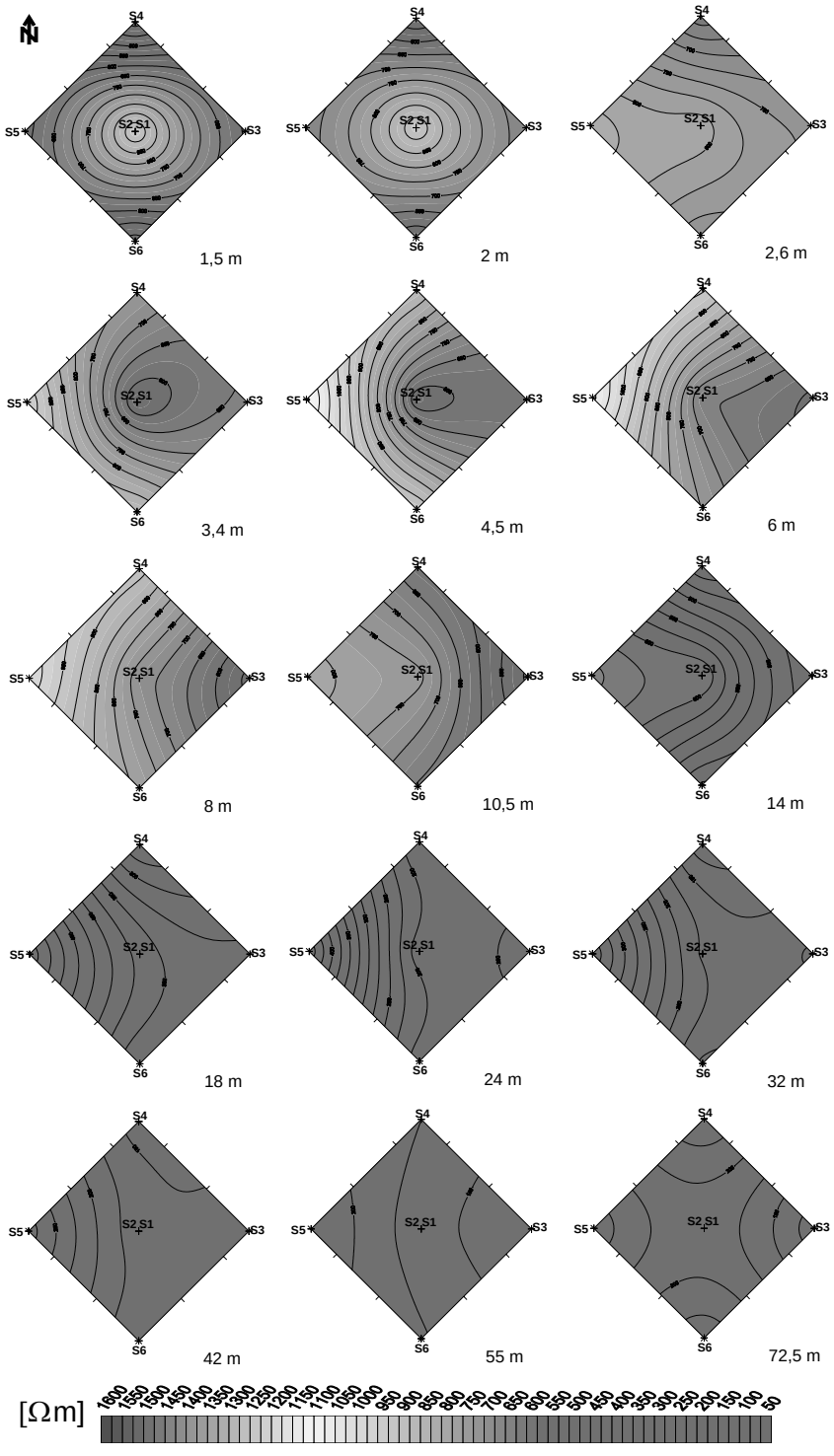


Fig. 7. Resistivity contour maps of the second series of measurements (winter).

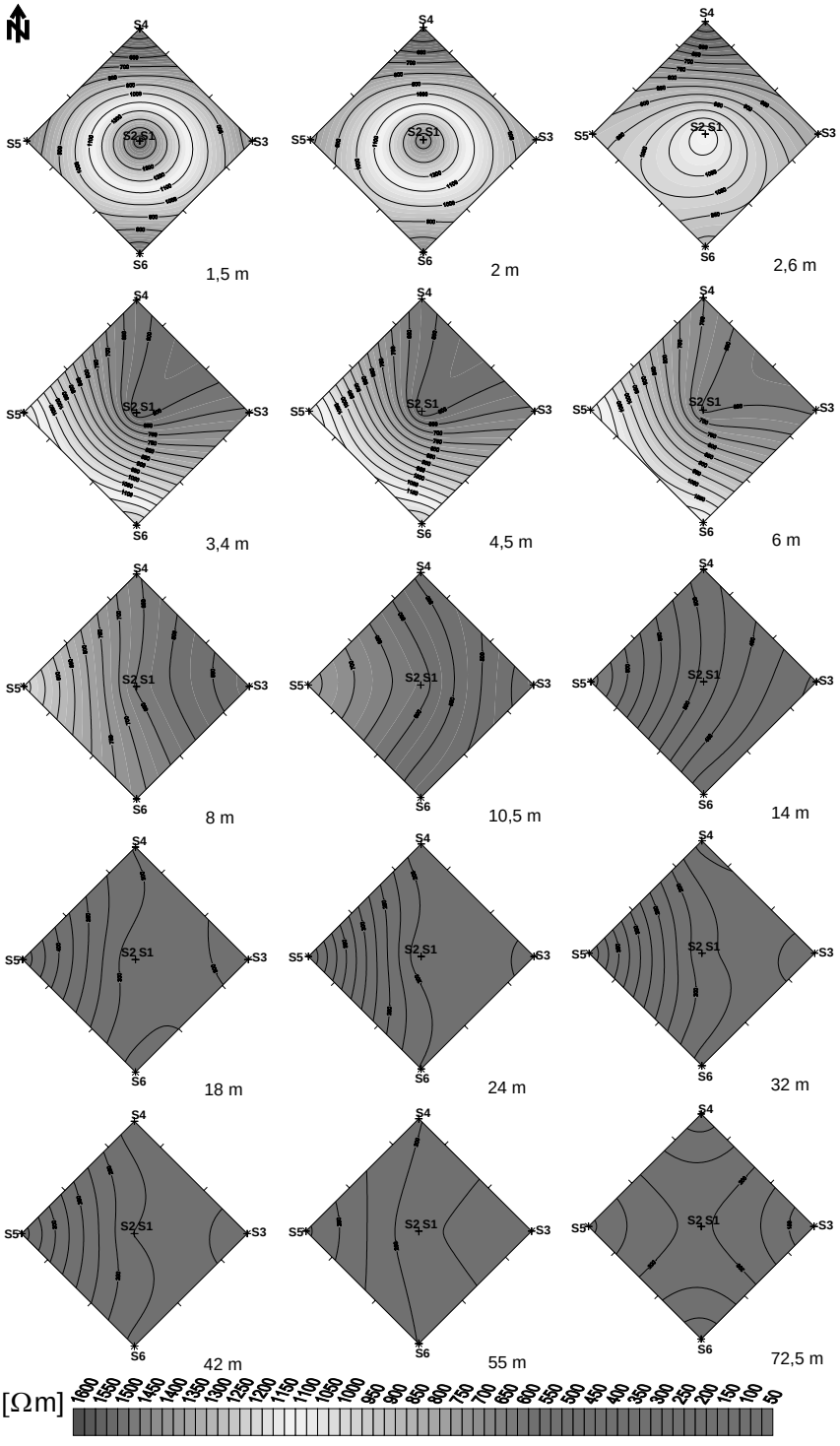


Fig. 8. Resistivity contour maps of the third series of measurements (spring).

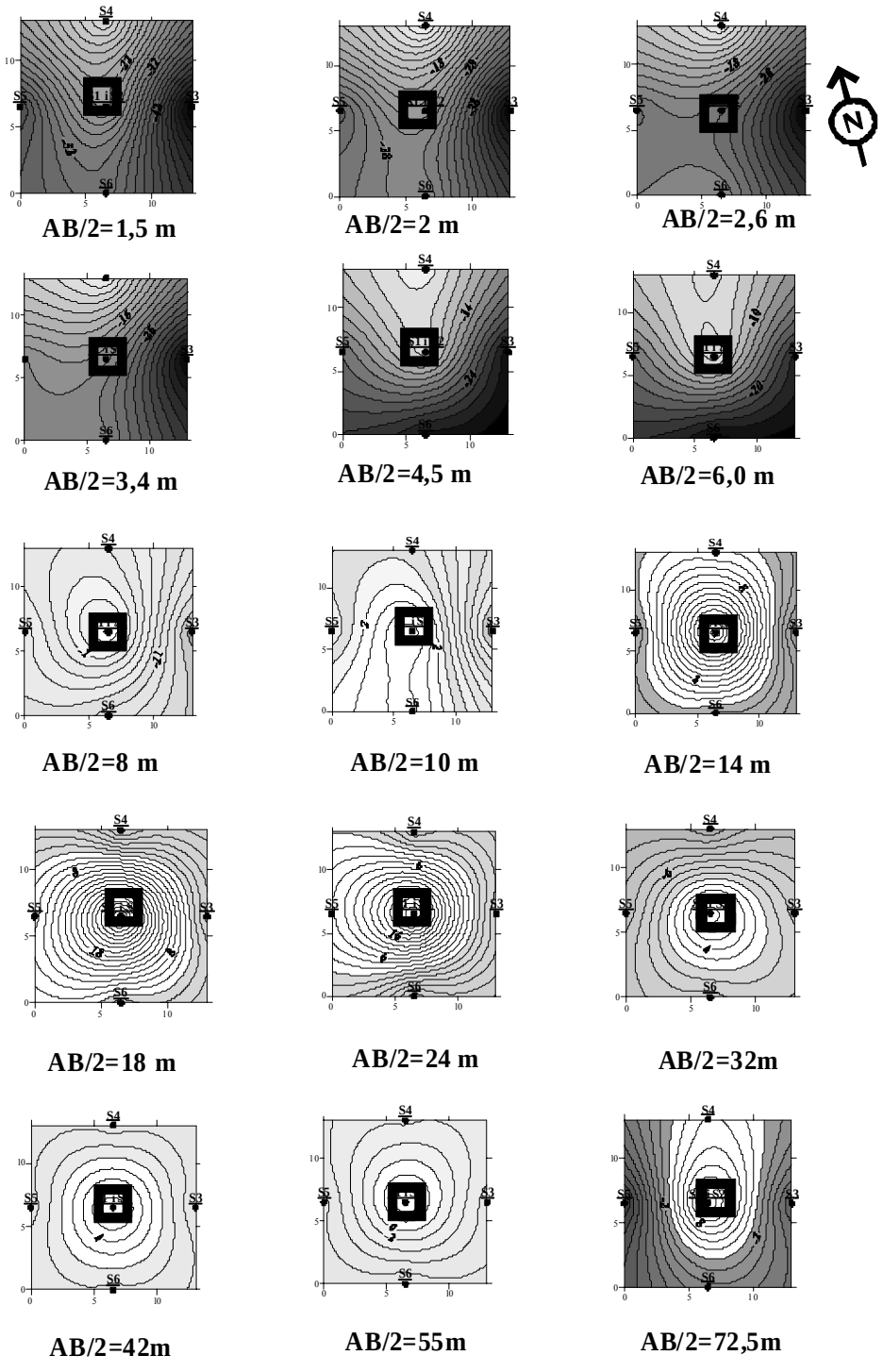


Fig. 9. Contour maps of the resistivity changes between second and first series of measurements (%) drawn in 2% intervals.

- The average change in resistivity value for given AB/2 from 4 points of soundings localized outside the shaft tube ($S_3$, $S_4$, $S_5$, $S_6$);
- The average change in resistivity value for given AB/2 from 2 points of soundings localized inside the shaft tube ($S_1$, $S_2$).

Results of calculations are plotted in Fig. 10. It can be observed that the resistivity changes in shaft's tube are higher than in rock strata. Especially significant changes occurred in second series of measurements in the range of 10–20 m of AB/2 spacing. The resistivity of that zone increased, which can be assigned to local mass disturbance, not observed in the next series. Nevertheless, in third data series it can be observed that the resitivity values increased moderately also in deeper parts of strata. This phenomena is visible more clearly, if the changes are shown for individual geoelectrical layers (Fig. 11).

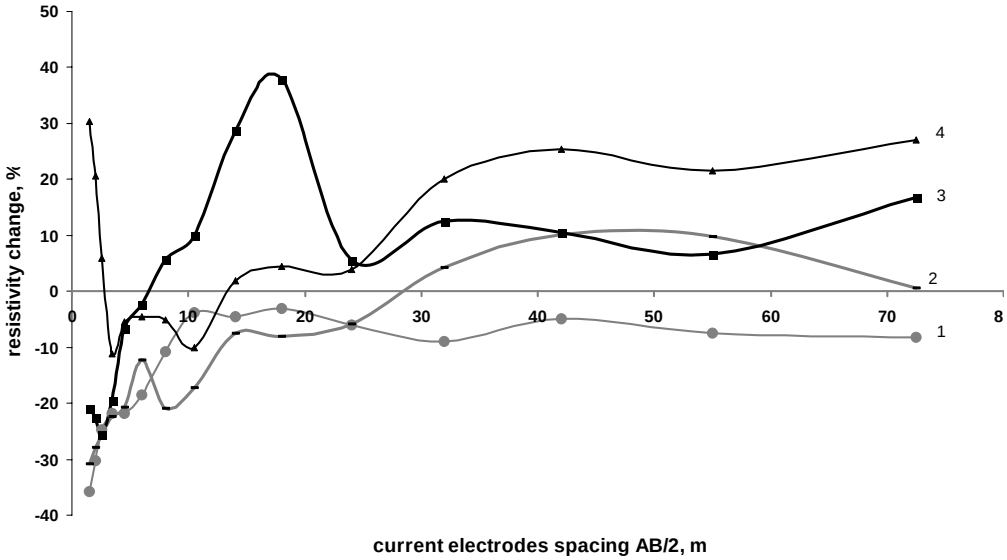


Fig. 10. Comparison of resistivity variations in shaft's tube and rock basement in relation to first series data as a function of current electrodes spacing (1, 2 – rock formation resitivity changes in series 2 and 3; 3, 4 – shaft's tube resitivity changes in series 2 and 3).

One should pay special attention to zones where the resistivity values increase. On the curve shown in Fig. 10, the zone has a form of local maximum in second/winter series in AB/2 range from 10 to 20 m (depth interval 4–8 m). In the established geoelectrical model of the medium, this interval corresponds to the weathered Triassic rocks layer. The observed changes of this layer resistivity are connected with lower watering in the period between first/autumn and second/winter series. It is also possible that part of material filling the shaft was washed out from this formation in the time interval between series 1 and 2 (the loosen ground zone was formed). At the same time, the increase of watering in the upper layer (embankments) has taken place what causes the soil particles to more downward. This anomaly was not recorded in

the third/spring series of measurements but an increase in resistivity of lower parts in shaft tube was observed, which is clearly seen in Fig. 11. Those changes indicate that within shaft's tube also mass transport phenomena have occurred.

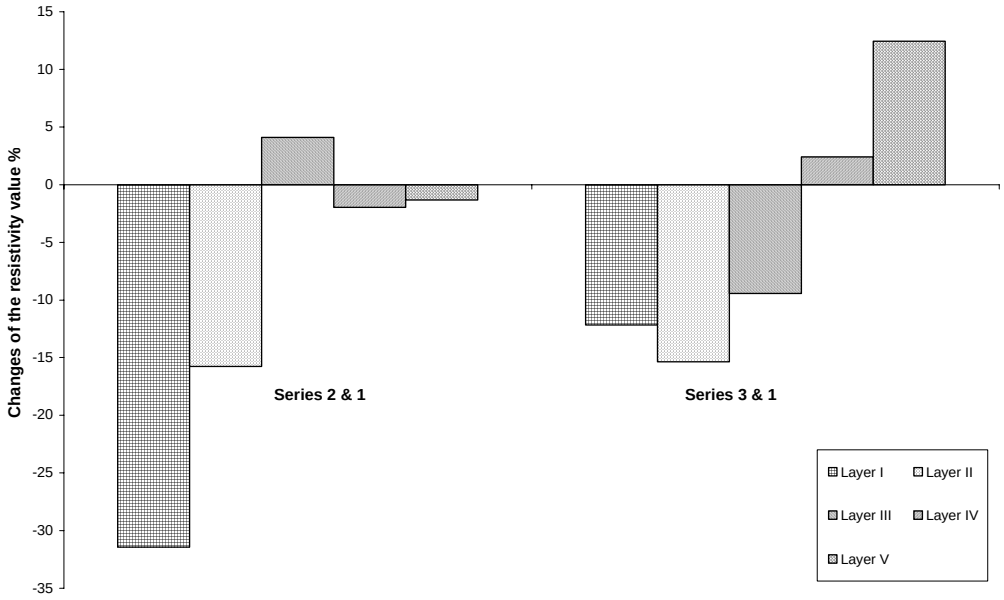


Fig. 11. Changes of the resistivity data recorded in series 2 and 3 in relation to data of the first series (%).

## 5. Conclusions

An analysis of test results shows that during the testing period relatively high quantitative changes took place in the subsurface zone of the studied area (AB/2 = 20 m, down to estimated depth of 8 m). The relative changes reached here the level of 35%. This value is close to the estimated fraction of rainfall which inflows to the geological environment impacted by mining operations. The amplitude of changes in the shaft tube is relatively higher but generally follows the trend of changes in the surrounding medium. All observations pointed out above indicate that within the boundaries of the test site, the cause of the surface deformation hazard is the washout and erosion phenomena taking place in shaft's tube material in accordance with hydrogeological model of the site. Hence, it should be noted that the depth of water table (estimated in preliminary interpretation of VES data) was not correct. This became obvious when the data of second series of measurements have been collected.

It can be also concluded that in contour maps of resistivity changes the shaft's tube is much better visible than in traditional resistivity isoohm maps. This conclusion can be used in methodology of geoelectrical measurements aimed for old shaft detection. The data sets gathered in two or more series of measurements can significantly reduce the interpretation errors.

The results of the study point out that the electric resistivity is a sensitive indicator of time dependent changes in medium and may be used to monitor various geodynamical processes in rock strata, in particular the surface deformation hazard over abandoned shafts. The temporary changes of rock resistivity reflect the precipitation rates in case of free percolation of water within the geological environment. If the percolation process induces mass movements, the above relation is disturbed, which can be detected by temporary or continuous geoelectrical measurements. For proper interpretation of geophysical data, an exact record of precipitation at the site has to be known.

## References


*Biuletyny IMGW*. Oddział w Katowicach. 2004-2005.

*Mapa hydrograficzna Polski w skali 1:50 000*. Arkusz 532.1. Jaworzno. Główny Urząd Geodezji i Kartografii. OPGK. Poznań 1986/1987.

Militzer, M., J. Schőn, U. Stotzner and R. Stoll, 1978, *Angewandte Geophysik*, VEB Deutscher Verlag fűr Grundstostoffindustrie, Leipzig.

Popiołek, E., Z. Pilecki, J. Ostrowski, J. Kłosiński, M. Koster, Z. Fajklewicz, A. Kotyrba, G. Mutke, E. Stewarski, A. Wróbel, J. Chodacki, Ł. Ortyl, J. Radomiński, R. Siata and A. Wójcik, 2005, *Ocena przydatności do zabudowy terenów zagrożonych deformacjami nieciągłymi za pomocą metod geofizycznych*, Wydawnictwo IGSMiE PAN, Kraków.

Sztelak, J., 1965, *Promień zasięgu drenażu wyrobisk górniczych lub ujęć wód podziemnych*, Rudy i Metale Nieżelazne nr. 3. Katowice.

Rogoż, M., 2004, *Hydrogeologia kopalniana z podstawami hydrogeologii ogólnej*. Główny Instytut Górnictwa, Katowice.



*Accepted 13 June 2006*